# A Regenerative Braking Strategy for Independently Driven Electric Wheel Accounting for Contemporary Use of Electric and Hydraulic Brakes

Michele Vignati(✉), Mattia Belloni, Edoardo Sabbioni, and Davide Tarsitano

Department of Mechanical Engineering, Politecnico di Milano, Via La Masa 1, 20156 Milan, Italy
michele.vignati@polimi.it

**Abstract.** The growth of electric mobility showed the possibility of reinventing the vehicle powertrain layout. The adoption of one motor per wheel allows to precisely control the driving and braking torque on each wheel. However, conventional friction brakes are necessary to guarantee top braking performance of the car since, in general, the braking toque by electric motor is not enough to perform maximum deceleration manoeuvres. A suitable blended braking distribution strategy must be designed to distribute the torques on the wheel by accounting for the vehicle state, the driver request, and the torque vectoring request by stability control algorithm. This paper presents and optimal control strategy that distributed the braking torques on the wheel accounting for electric and hydraulic brakes. The control algorithm considers than the regulations requirements, the wheel vertical load condition both in longitudinal and lateral dynamics conditions, and the request by driver and stability control.

**Keywords:** Braking strategy · Braking repartition · Torque vectoring · Vehicle control

## 1 Introduction

Due to climate changes, and the growing interest in the production of less pollutant vehicles, in recent years, the development of electric vehicles (EVs) has undergone an exponential growth. The introduction of electric motors (EMs), in fact, leads to the possibility of reinventing the traditional powertrain using multiple motors, controlling the torque at each wheel independently, and eluding transmissions or differentials. EMs have a quicker response with respect to the traditional internal combustion engine (ICE), can be easily managed, and are able, by regenerative braking, to provide negative torque to the wheels recovering part of the vehicle kinetic energy during decelerating manoeuvres. Having more than one EM, one per wheel (e.g. In-Wheel-Motors - IWM), it is possible to have some torque vectoring on the vehicle controlling the torque at each wheel [1–3]. Due to higher promptness of EMs with respect the traditional oil-actuated friction brakes,


A. Orlova and D. Cole (Eds.): IAVSD 2021, LNME, pp. 1256–1268, 2022.
https://doi.org/10.1007/978-3-031-07305-2_116

it is also possible to reinvent the anti-lock braking system (ABS), reducing in this way the stopping distance of the vehicle during the panic braking manoeuvres [4]. However, besides the EMs can provide negative torque, the traditional mechanical hydraulic brakes (HB) are still necessary since EMs are not able to generate sufficient negative torque at any vehicle velocity. An EV is usually equipped with the EMs, an energy storage system (battery and supercapacitors) and power converters. In case of failure of one of these components, or in case the energy regenerated during braking manoeuvre cannot be stored into the batteries and cannot be dissipated (for example because energy storage system is fully charged), the HB implant it is necessary for safety reasons. Then, having the possibility to actuate negative torque to the wheels using both the EM as a generator, and the traditional HB it is needed a smart braking control strategy that considers the system parameters (wheel peripheral speeds, motor efficiency, load transfers, battery Status Of Charge (SOC), etc.) and optimize the energy regeneration.

In most independent wheel electric vehicles (IWEV) hierarchical controls are adopted: the driver steer command inputs into vehicle while accelerator and brake pedal inputs are processed by VCU to generate total driving and braking torque requested by the driver. Then a stability control based on TV generates a request of total yaw moment to stabilize or improve the performance of the car. These two contributions must be developed thanks to a suitable torque distribution strategy.

Considering EMs and HB, the braking system becomes a multi-input plant. The problem is usually treated considering three main subproblems: front-rear axle brake repartition, electrical-mechanical brake repartition at each wheel and electric power management. [5] provides an analysis different battery/supercapacitor EV's hybrid systems, while [6–9] present different lithium-ion battery models for automotive applications. A control logic for hybridized vehicle equipped with IWMs is suggested in [10]. The authors in [11] use as a design variable the front-rear brake distribution and the electro-mechanical torque repartition and solve the braking repartition problem by a deep learning optimization algorithm. In [12] the algorithm proposed maximize the electric braking torque using wheel speed and battery SOC as key parameters. The strategy proposed in [13] uses a fixed front-rear repartition that favourites the front axle braking force using the maximum motor torque available (as function of vehicle speed). [14] splits the torque between the front and rear axle using the ideal torque distribution, and distributes the electro-mechanical torque at each wheel using a fuzzy logic controller based on torque variation rate and battery SOC. In [15] it is used the optimal control strategy in which an MPC minimize a cost functional that involves the optimal front-rear force repartition, the torque required by the driver, the efficiency of EM and the HB. Most of the papers reported here do not consider the lateral vehicle dynamic but focuses on conditions in which the vehicle is in pure straight driving condition, neglecting in this way the lateral vehicle dynamics.

Other papers which consider car lateral dynamics are instead neglecting the blended braking condition. E.g. [16] proposes an optimized control strategy for IWM vehicle which considers vehicle lateral stability. [17] proposes an optimal control distribution strategy for IWM vehicle considering energy efficiency. Both papers do not consider blended braking conditions.

To account for both blended braking and car longitudinal and lateral dynamics an optimized distribution algorithm is presented in this paper. The optimal problem maximizes the recovered energy by accounting for EMs and HBs while considering the wheel applicable torque due to friction limitation by computing the normal load on the wheel due to longitudinal and lateral load transfers. The optimal problem is solved offline, reducing the computational time required while running, then look-up tables are generated. The control strategy has been tested in several simulations both in pure straight driving and in cornering conditions.

## 2 Torque Distribution Algorithm

Torque distribution algorithm is taken from [18] and here briefly summarised. The overall scheme of the controller is reported in Fig. 1. Given the driver required torque and the TV required yaw moment, the controller distribute torques between EMs and HB accounting for vehicle longitudinal and lateral dynamics.

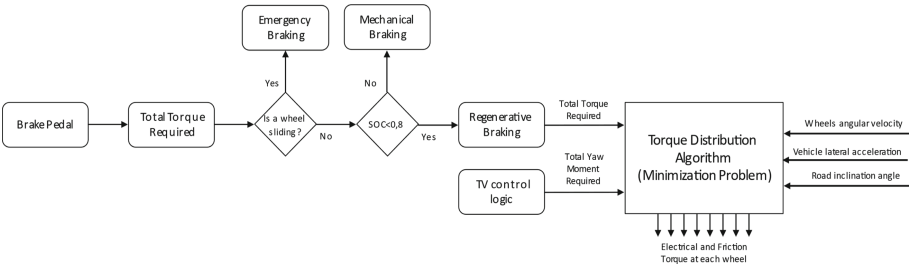


**Fig. 1.** Scheme of the braking algorithm.

The algorithm maximizes the recovered energy by EMs while braking. The following quantity is thus minimized

$$\min \left[ \sum_{j=FR,FL,RR,RL} T_{E,j} \cdot \omega_j \cdot \eta(T_{E,j}, \omega_j) \right] \tag{1}$$

where, considering the j-th wheel, $T_{E,j}$ is the electric torque, $\omega_j$ the angular speed, $\eta$ is the EM efficiency which is a function of motor torque and speed according to motor efficiency map reported in Fig. 2.

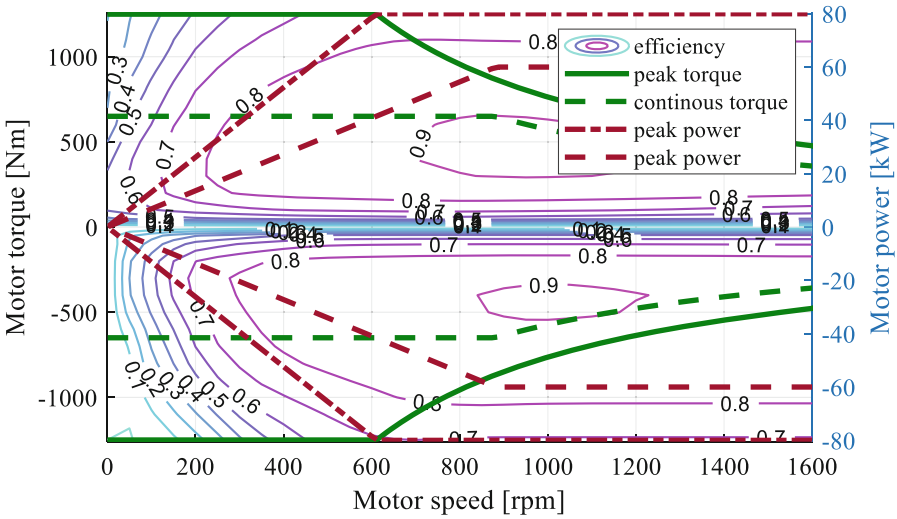


**Fig. 2.** In-wheel motor torque characteristic (in green). Contour map refers to motor efficiency.

The design variables correspond to the electric and friction torques generated respectively by EMs and traditional brakes:

$$T_{i,j} \quad \text{where: } i = \{E, F\} \text{ and } j = \{FR, FL, RR, RL\} \tag{2}$$

Considering the four wheels of the vehicle, the design variables are eight. The goal of the optimization problem is to maximize the power recovered during braking manoeuvre as shown in Eq. (1).

To account for driver and TV requests, equality constraints must be satisfied. The total torque on the vehicle must be equal to driver required torque

$$T_{\text{Req}} = \sum\nolimits_{j=FR,FL,RR,RL} T_{E,j} + T_{F,j} \tag{3}$$

while the total yaw moment on the car must be equal to the one demanded by TV stability control

$$M_{Z,Req} = \left(\left(T_{E,FL} + T_{F,FL}\right) - \left(T_{E,FR} + T_{F,FR}\right)\right)\frac{c_F}{2R_w} + \left(\left(T_{E,FL} + T_{F,FL}\right) - \left(T_{E,FR} + T_{F,FR}\right)\right)\frac{c_R}{2R_w} \tag{4}$$

The physical limitations of the torque actuation systems are then considered. HB torque is lower limited by maximum braking pressure and upper limited to zero. EM torque is limited by motor characteristic as reported in Fig. 2.

Actuator limits are not the only factors limiting the exploitable torque on the wheel. Adhesion limit must be considered:

$$\left|T_{E,j} + T_{F,j}\right| \leq \mu F_{Z,j} R_w \quad \text{where: } j = \{FR, FL, RR, RL\} \tag{5}$$

where $\mu$ is the tire-road friction coefficient, $R_w$ the wheel radius, and $F_{Z,j}$ the vertical load on the wheel which is computed according to the following equations:

$$\begin{aligned} F_{z,FR} &= \frac{mg}{2}\left(\frac{l_R}{l} - \frac{A_{xReq}h_G}{gl} - \frac{2h_G A_y}{c_F g}\left(\frac{K_{\rho F}}{K_{\rho F}+K_{\rho R}}\right)\right) \\ F_{z,FL} &= \frac{mg}{2}\left(\frac{l_R}{l} - \frac{A_{xReq}h_G}{gl} + \frac{2h_G A_y}{c_F g}\left(\frac{K_{\rho F}}{K_{\rho F}+K_{\rho R}}\right)\right) \\ F_{z,RR} &= \frac{mg}{2}\left(\frac{l_F}{l} + \frac{A_{xReq}h_G}{gl} - \frac{2h_G A_y}{c_R g}\left(\frac{K_{\rho R}}{K_{\rho F}+K_{\rho R}}\right)\right) \\ F_{z,RL} &= \frac{mg}{2}\left(\frac{l_F}{l} + \frac{A_{xReq}h_G}{gl} + \frac{2h_G A_y}{c_R g}\left(\frac{K_{\rho R}}{K_{\rho F}+K_{\rho R}}\right)\right) \end{aligned} \tag{6}$$

where longitudinal and lateral load transfers are accounted thanks to longitudinal and lateral accelerations ($A_x$ *and* $A_y$). In Eq. (6), $h_G$ is the vehicle center of mass (c.o.m.) heigh from ground; $c_F$ and $c_R$ the front and rear axle track width; $l$ the wheel base; $l_F$ and $l_R$ the distances of vehicle c.o.m. from front and rear axle respectively; $K_{\rho F}$ and $K_{\rho R}$ are the roll stiffnesses of the front and rear axle. The lateral acceleration $A_y$ can be directly measured with an accelerometer on the vehicle, instead the longitudinal acceleration $A_x$ is calculated considering the required driver's input by a longitudinal force equilibrium on the vehicle and the wheels combined friction limit:

$$A_{xReq} = min\left[\frac{1}{m}\left(\frac{T_{Req}}{R_w} - F_{res}\right), -\sqrt{(\mu g)^2 - {A_y}^2}\right] \tag{7}$$

Finally, the European regulation ECE-R13 [25] defines the maximum and minimum force that must be transmitted to the ground by the rear axle wheels as function to the front axle one. This limitation can be written in the following form

$$\left|\frac{\sum_{j=FR,FL,RR,RL} T_{E,j} + T_{F,j}}{R_w}\right| \geq 0.1 + 0.85(\mu - 0.2) \tag{8}$$

## 3 Minimization Problem Numerical Results

The multi-input problem can be solved offline collecting results in look-up tables. The considered discretization of the input parameters is reported in Table 1.

**Table 1.** External parameters discretization for minimization problem

| Variable | Symbol | Min value | Max value | Unit | Points |
|---|---|---|---|---|---|
| Driver required torque | $T_{req}$ | −4000 | 0 | Nm | 21 |
| Wheel/motor angular velocity | $\omega_w$ | 0 | 1600 | rpm | 21 |
| Yaw moment required | $M_{z,req}$ | −1500 | 1500 | Nm | 11 |
| Lateral acceleration | $A_y$ | −g | g | $m/s^2$ | 11 |

The parameter discretization considers the most common driving conditions; the maximum and minimum torque required guarantee a vehicle deceleration of about 6 $m/s^2$

on dry asphalt ($\mu = 0.9$). The wheel angular speed considers the EMs limits, and the lateral acceleration considers the friction ellipse limit.

Matlab function "*fmincon*" with "Sqp" method is used to solve the constrained minimization problem. Results are stored in lookup tables.

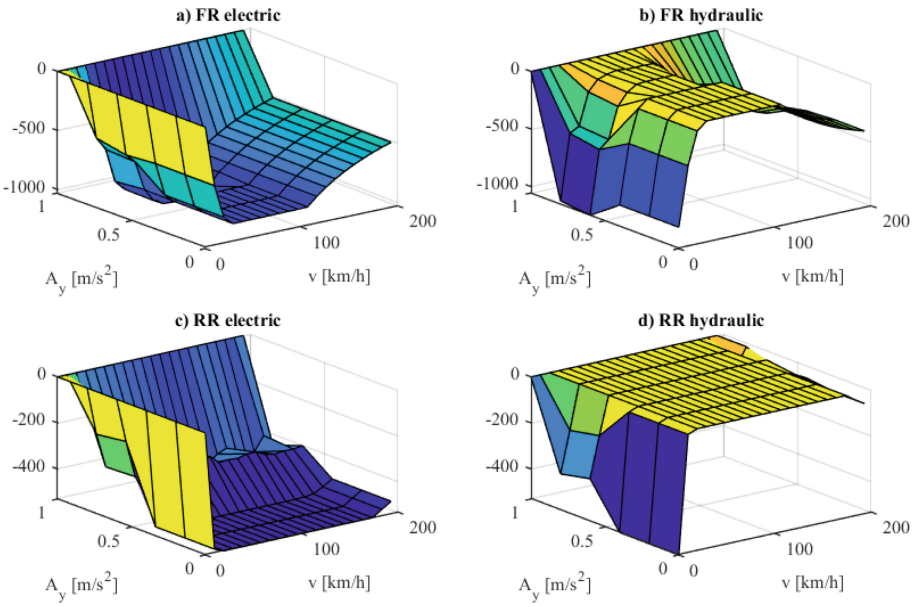


**Fig. 3.** Electric and hydraulic braking torque (a, c and b, d respectively) distribution on the front and rear right (a, b and c, d respectively) wheel as function of vehicle speed v and lateral acceleration $A_y$: $M_{z,req} = 0$, $T_{req} = -2800$ Nm.

As an example, Fig. 3 represents the solution of the minimization problem for front right (FR) and rear right (RR) wheel for different vehicle speeds (v) and different lateral accelerations ($A_y$) when a constant braking torque is required by driver of 2800 Nm.

Looking at Fig. 3a, which represents the electric braking torque on front right (FR) wheel, it is possible to notice the speed dependency of the applied torque. The torque limitation due to motor characteristic torque (Fig. 2) is clearly visible for speed higher than 100 km/h and for very low speed where the motor efficiency is very low. Looking at Fig. 3b it is clear the compensation of the wheel torque by hydraulic brakes. The required hydraulic brake torque is in fact complementary to the electric torque thus to have an almost constant total braking torque on FR wheel.

Torque required to rear right (RR) wheel are depicted in Fig. 3c and Fig. 3d which report the electric and hydraulic braking torques, respectively. From Fig. 3d it is possible to notice that the hydraulic brakes are practically not used for this level of required total braking torque. This is because the electric torque is enough to brake the rear wheels that, in general, are braked with smaller torque due to longitudinal load transfer. Hydraulic brakes are in fact compensating the pure efficiency of EM at very low speed (smaller than 5 km/h).

Comparing Fig. 3a and Fig. 3c it is possible to notice the influence of lateral acceleration on front-rear distribution. When $A_y$ increases the load transfer is higher on rear wheels because of the rolling stiffness characteristic of the selected car. Since the RR wheel normal load reduces more than the FR one, the braking torque on FR is increased and RR reduced.

## 4 Simulation Results

The distribution control strategy is tested in Matlab/Simulink simulation environment. A 14 d.o.f. model (ViCar realtime) of a segment D passengers' car is used. It accounts for three displacements of the vehicle centre of mass (c.o.m.), three rotations of the car body (yaw, pitch, and roll), four vertical displacements of unsprang masses, and four wheels angular velocities about hub axis. The four EMs are modelled considering the torque-speed characteristic, shown in Fig. 2, and considering an equivalent first-order time lag transfer function with the same bandwidth of real motors to reproduce the dynamics of the motor torque regulator. The HB are modelled considering pressure to torque gain $K_b$ accounting for effective disk radius, pad-disk friction etc… The dynamics of the oil pressure at the brake calliper is expressed by a second order transfer function considering oil pump and circuit dynamics.

Torque vectoring control strategy generates a yaw moment $M_{Z,req}$ that stabilize the vehicle and improves its performances by tracking yaw rate and sideslip angle references. It is based on a proportional controller on the vehicle yaw rate $\dot{\psi}$ and vehicle sideslip angle $\beta$ as shown in [19].

To compare the new torque control logic, two alternatives control logics have been implemented in the following logic A and B while the control strategy presented in the previous paragraph will be referred as strategy C. The strategy A (blue line in Fig. 4) exploits a proportional front-rear brake repartition. This distribution is usually adopted in vehicles with mechanical brake distributor in which the front to rear repartition is fixed. In this case, the proportionality coefficient is equal to the ratio between the rear and the front brake equivalent coefficients ($K_{b,F}$ *and* $K_{b,R}$ respectively) until the force at the rear axle does not overcome the limit of ideal force distribution. Then the torque distribution at the rear axle remains constant for any value of torque required, and only the force at the front axle increases. Transition from linear to constant rear axle torque corresponds to front-rear distribution value when the proportional curve intersects the ideal braking distribution (see Fig. 4). The strategy B exploits the ideal front-rear toque distribution (red line in Fig. 4). This repartition is the most used in literature ([14, 20–23]) because it guarantees the minimum stopping distance, increasing the braking performances.

For both strategies, the total braking torque required is provided by the braking system exploiting the electric braking torque until the motor limit is reached then the remaining demanded torque is provided by friction brakes.

The yaw moment necessary to satisfy the TV request is split front to rear according to the front to rear distribution strategy. Then each wheel contributes generating half of the total yaw moment required at the respective axle.

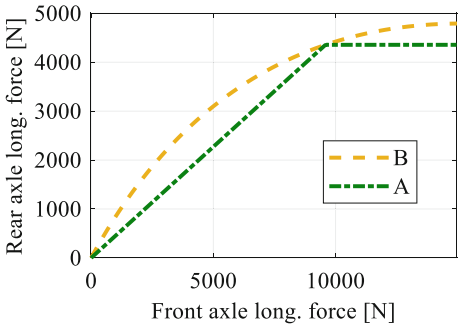


**Fig. 4.** Strategies A and B, front to rear torque distribution. (Color figure online)

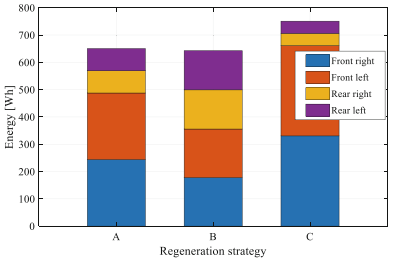


**Fig. 5.** WLTP driving cycles energy regenerated for each wheel

### 4.1 WLTP Driving Cycle

To analyse the controls performance in straight driving, the WLTP urban driving cycles was simulated. The tests have been performed using the vehicle model described above and using a PI controller on vehicle speed to make the vehicle follow the velocity profile. Since the attention is posed on the braking phase, the driving distribution strategy is the same for the three logics and its performance is not considered here.

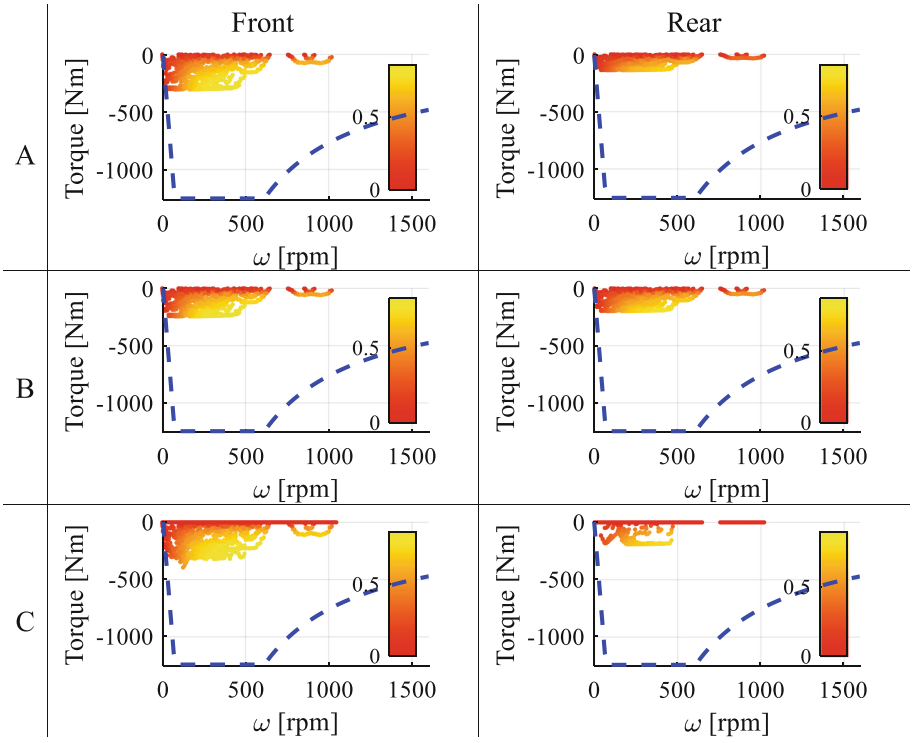


**Fig. 6.** Motor torque and efficiency vs speed during the WLTP cycle for front and rear wheels: logic A, B, and C.

Figure 5 reports the total energy recovered from electric motors in the WLTP driving cycle, by reporting the contribution of each wheel. The deceleration during the driving cycle is always below to 1.5 m/s$^2$. This means that also the required braking torque is small if compared to the motor top performance. At small braking torques, a control strategy accounting for motor efficiency can show great benefits. In fact, the energy recovered from strategy C is considerably higher than strategies A and B. Strategy C recovers 15% more than strategy A and 17% more than strategy B. This happens because strategy C prefers to brake with only one axle thus increasing the demanded braking torque which makes the motors to work in a better working range. Figure 6 shows the working range of front and rear wheels for the three strategies. The colour of the points in the graph refers to the motor efficiency. Again, it is possible to see how the strategy C is preferring to use only front axle to maximize the motor efficiency.

### 4.2 Braking in a Turn Manoeuvre

The brake in turn is a manoeuvre to test vehicle lateral stability and it is standardized in ISO 7975:2006(E). The vehicle enters a turn with a constant fixed steering angle. When steady-state conditions are reached, a braking torque is demanded. The combined

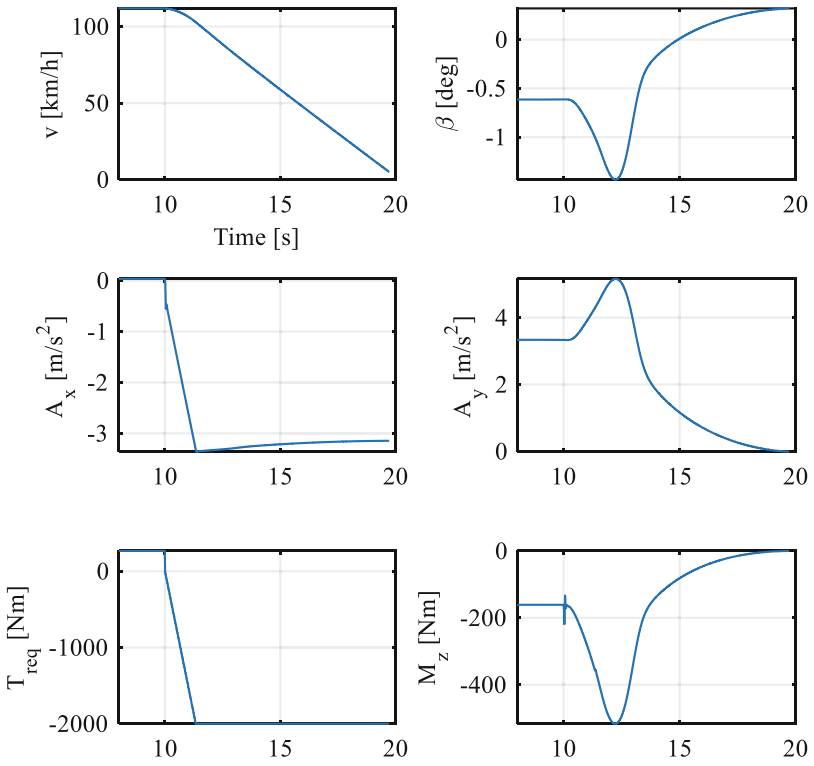


**Fig. 7.** Braking in a turn maneuver. Vehicle speed (v), sideslip angle (β), accelerations (Ax and Ay), required torque (Treq) by driver, and TV yaw moment (Mz).

longitudinal and lateral acceleration stresses the vehicle dynamics and may lead to instability. Under this condition it is in general necessary to limit the sideslip angle which can be done by applying torque vectoring. Figure 7 reports the principal quantity necessary to understand the manoeuvre. The steering angle is constant and equal to 11°. The vehicle initial speed is 110 km/h which results in a steady-state lateral acceleration of about 3.5 m/s$^2$. Then a constant braking torque is required by the driver of about 2000 Nm. Under these conditions, the resulting longitudinal acceleration is about 3.5 m/s$^2$. Vehicle dynamics, i.e. the sideslip angle increase, makes the TV control to generate a yaw moment to improve the car stability. For sake of clarity, figure reports only one line per each quantity, relative to vehicle C, because the vehicle behaviour with logic A, B, and C is so close that no differences can be perceived. This is reasonable since the vehicle dynamics is mostly affected by driver commands and TV yaw moment while the distribution strategy can only marginally affect the vehicle behaviour.

The effect of distribution control strategies can instead be appreciated by looking at the torque on each single wheel and the energy recovery efficiency.

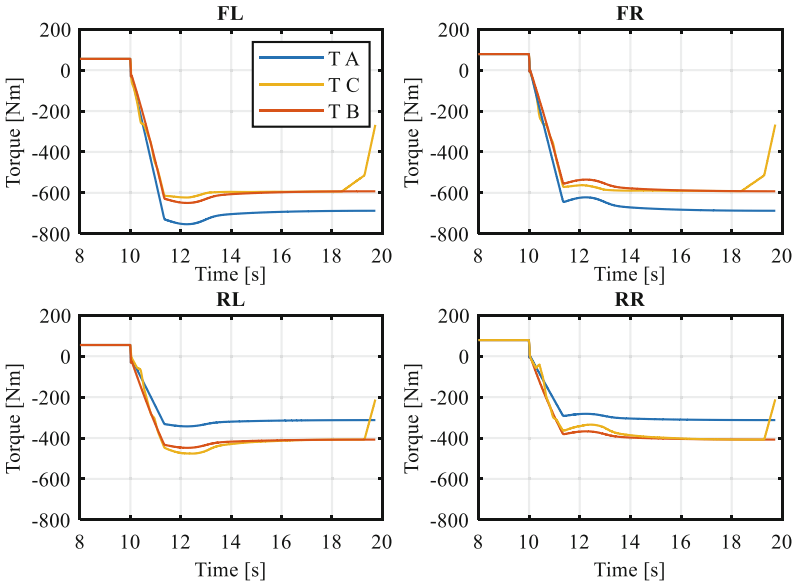


**Fig. 8.** Torques on wheels for vehicle A, B, and C in braking in a turn maneuver.

Figure 8 reports the electric torques applied on each wheel for the three considered vehicles. Like previously shown results, the front to rear torque distribution is different for the three control strategies. Logic A uses more the front axle than the rear, while logic B and C are comparable. Differences between B and C can be noticed around second 12 where the yaw moment required by TV is maximum. In this condition logic C prefers to have more yaw moment on the rear axle than on the front. For all the considered vehicles, in these conditions, HB are not used since braking performance of EMs are enough to deploy the required braking torque.

Figure 9 reports the total recovered energy during the braking in a turn manoeuvre. Logic A is the one that recovers less energy while performance of logic B and C are comparable. Still logic C shows higher recovered energy. This is due to the nature of the simulated manoeuvre since almost constant torque is required by driver. A variability of the required torque may show different performance are shows in WLTP simulation.

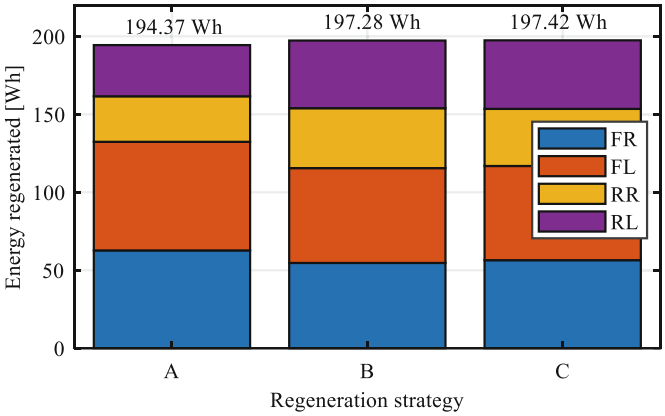


**Fig. 9.** Energy recovered in braking in a turn maneuver for the three considered control strategies A, B, and C.

## 5 Conclusions

This paper presents an optimal distribution strategy that distributed braking torques on wheels for electric vehicles with independently driven wheels considering both electric and hydraulic brakes. The control strategy maximizes the recover energy by considering the electric motors efficiency map. Constraints are the total braking torque required by driver and the total yaw moment required by torque vectoring stability control. Furthermore, the algorithm considers friction limitation on the wheel by considering the normal load due to longitudinal and lateral load transfers.

Proposed algorithm is compared to other taken from literature by means of numerical simulations. Results show the superior performance of the proposed algorithm in particular at low speeds where a correct use of the motor allows to improve the overall efficiency.

## References

1. Braghin, F., Sabbioni, E., Sironi, G., Vignati, M.: A feedback control strategy for torque-vectoring of IWM vehicles. In: Proceedings of the ASME Design Engineering Technical Conference, vol. 3 (2014). https://doi.org/10.1115/DETC2014-34372
2. Vignati, M., Sabbioni, E., Cheli, F.: A torque vectoring control for enhancing vehicle performance in drifting. Electronics (Switzerland) **7**(12) (2018). https://doi.org/10.3390/electronics7120394. Art. no. 394

3. Vignati, M., Sabbioni, E.: Force-based braking control algorithm for vehicles with electric motors. Veh. Syst. Dyn. **58**(9), 1348–1366 (2020)
4. Kouchachvili, L., Yaïci, W., Entchev, E.: Hybrid battery/supercapacitor energy storage system for electric vehicles. J. Power Sources **374**, 237–248 (2018)
5. Taici, W., Kouchachvili, L., Entchev, E.: Dynamic simulation of battery/supercapacitor hybrid energy storage system for electric vehicles. In: 8th International Conference on Renewable Energy Research and Applications, Brasov, ROMANIA, 3–6 November 2019
6. Mousavi, S.M., Nikdel, G.M.: Various battery models for various simulation studies and applications. Renew. Sustain. Energy Rev. **32**, 477–485 (2014)
7. Fotouhi, A., Auger, D.J., Propp, K., Longo, S., Wild, M.: A review on electric vehicle battery modelling: from lithium-ion toward lithium-sulphur. Renew. Sustain. Energy Rev. **56**, 1008–1021 (2016)
8. Damiano, A., Musio, C., Marongiu, I.: Experimental validation of a dynamic energy model of a battery electric vehicle. In: 4th International Conference on Renewable Energy Research and applications, Palermo, Italy, 22–25 November 2015
9. Grandone, M., Naddeo, N., Marra, D., Rizzo, G.: Development of a regenerative braking control strategy for hybridized solar vehicle. IFAC-PapersOnLine **49–11**, 497–504 (2016)
10. He, C., Wang, G., Gong, Z., Xing, Z., Xu, D.: A control algorithm for the novel regenerative-mechanical coupled brake system with by-wire based on multidisciplinary design optimization for an electric vehicle. Energies **11**, 2322 (2018). https://doi.org/10.3390/en11092322
11. Valentin, I., Javier, O., Thomas, P., Frank, B., Dzmitry, S., Barys, S.: Electric and friction braking control system for AWD electric vehicles. F2014-Special Session 'Vehicle Dynamics Control for Fully Electric Vehicles – Outcomes of the European Project E-VECTOORC'
12. Lv, C., Zhang, J., Li, Y., Yuan, Y.: Regenerative braking control algorithm for an electrified vehicle equipped with a by-wire brake system. SAE Technical Paper 2014-01-1791 (2014). https://doi.org/10.4271/2014-01-1791
13. Zhou, Z., Mi, C., Zhang, G.: Integrated control of electromechanical braking and regenerative braking in plug-in hybrid electric vehicles. Int. J. Veh. Des. **58**(2/3/4) (2012)
14. Xu, W., Chen, H., Zhao, H., Ren, B.: Torque optimization control for electric vehicles with four in-wheel motors equipped with regenerative braking system. Mechatronics **57**, 95–108 (2019)
15. Zhang, X., Wei, K., Yuan, X., Tang, Y.: Optimal torque distribution for the stability improvement of a four-wheel distributed-driven electric vehicle using coordinated control. J. Comput. Nonlinear Dyn. **11**(5) (2016). https://doi.org/10.1115/1.4033004. Art. no. 051017
16. Guo, L., Lin, X., Ge, P., Qiao, Y., Xu, L., Li, J.: Torque distribution for electric vehicle with four in-wheel motors by considering energy optimization and dynamics performance. In: IEEE Intelligent Vehicles Symposium, Proceedings, pp. 1619–1624 (2017). https://doi.org/10.1109/IVS.2017.7995941. Art. no. 7995941
17. Vignati, M., Belloni, M., Tarsitano, D., Sabbioni, E.: Optimal cooperative brake distribution strategy for IWM vehicle accounting for electric and friction braking torques. Math. Probl. Eng. **2021**, 19 pages (2021). https://doi.org/10.1155/2021/1088805. Article ID 1088805
18. Vignati, M., Sabbioni, E.: A cooperative control strategy for yaw rate and sideslip angle control combining torque vectoring with rear wheel steering. Veh. Syst. Dyn. (2021). https://doi.org/10.1080/00423114.2020.1869273
19. De Novellis, L., Sorniotti, A., Gruber, P.: Optimal wheel torque distribution for a four-wheel-drive fully electric vehicle. SAE Int. J. Passenger Cars Mech. Syst. **6**(1), 128–136 (2013). https://doi.org/10.4271/2013-01-0673. Cited 42 times
20. Lv, C., Zhang, J., Li, Y., Yuan, Y.: Regenerative braking control algorithm for an electrified vehicle equipped with a by-wire brake system. SAE Technical Paper 2014-01-1791 (2014). https://doi.org/10.4271/2014-01-1791

21. Zhou, Z., Mi, C., Zhang, G.: Integrated control of electromechanical braking and regenerative braking in plug-in hybrid electric vehicles. Int. J. Veh. Des. **58**(2/3/4), 223–239 (2012)
22. Gao, Y., Ehsani, M.: Electronic braking system of EV and HEV—integration of regenerative braking, automatic braking force control and ABS. SAE Trans. **110**, 576–582 (2001). Section 7: Journal of Passenger Cars: Electronic and Electrical Systems
23. Ko, J., Ko, S., Son, H., Yoo, B., Cheon, J., Kim, H.: Development of a brake system and regenerative braking cooperative control algorithm for automatic-transmission-based hybrid electric vehicles. IEEE Trans. Veh. Technol. **64**(2), 431–440 (2015)